Ab Initio Study of the Exchange Coupling in Oxalato-Bridged Cu(II) Dinuclear Complexes

J. Cabrero,[†] N. Ben Amor,[†,‡] C. de Graaf,[§] F. Illas,[§] and R. Caballol*[,†]

Departament de Química Física i Inorgànica and Institut d'Estudis Avançats, Universitat Rovira i Virgili, Pl. Imperial Tarraco, 1. 43005 Tarragona, Spain, and Departament de Química Física and Centre de Recerca en Química Teòrica, Universitat de Barcelona, Martí i Franquès, 1. 08017 Barcelona, Spain

Received: May 24, 2000; In Final Form: August 15, 2000

The structural dependence of the coupling constant in a series of $[L_3Cu(\mu\text{-}C_2O_4)CuL_3]^{2+}$complexes is analyzed by means of ab initio difference-dedicated configuration interaction (DDCI2) calculations on the model (μ-oxalato)bis[triamminecopper(II)] cation, $[(NH_3)_6Cu_2(\mu\text{-}C_2O_4)]^{2+}$, in which the nitrogen-coordinated ligands have been substituted by NH_3. Two types of geometrical structures have been considered: three different C_{2h} geometries and four crystallographic centrosymmetric geometries taken from $[(Et_5dien)_2Cu_2(\mu\text{-}C_2O_4)](BPh_4)_2$ and $[(Et_5dien)_2Cu_2(\mu\text{-}C_2O_4)](PF_6)_2$ (Et_5dien = 1,1,4,7,7-pentaethyldiethylenetriamine), $[(tmen,2\text{-}MeIm)_2Cu_2(\mu\text{-}C_2O_4)](PF_6)_2$ (tmen = *N*,*N*,*N*′,*N*′-tetramethylethylenediamine and 2-MeIm = 2-methylimidazole), and $[(dien)_2Cu_2(\mu\text{-}C_2O_4)](ClO_4)_2$ (dien = diethylenetriamine). The results show that the antiferromagnetic coupling is strongly underestimated when pure DDCI2 calculations are performed, but when the CI space includes the relaxation of the oxalato-copper charge transfer, quantitative agreement with the experimental results is reached with an error smaller than 5 cm^{-1}. The role of the external ligands in the model is also discussed by means of broken symmetry DFT calculations. At this level of theory, a very different influence of the ligands is predicted by different exchange-correlation functionals. Therefore, the use of DFT to investigate this effect should be considered with caution.

1. Introduction

Among the large number of transition metal polynuclear complexes with weak interactions between the metallic centers, many bridged copper Cu(II) binuclear compounds with a wide variety of bridging ligands (chloro,[1] azido,[2] hydroxo,[3] oxalato,[4] etc.) have been described that show a strong dependence between the magnetic behavior and the structural factors such as the copper coordination, the nature of the external ligands, the geometrical structure of the Cu−bridge−Cu unit, etc. From the early seventies[5,6] successful qualitative interpretations of the magneto-structural correlations were established for copper dimers. In the eighties, first quantitative approaches to evaluate the exchange coupling constant also dealt with copper binuclear complexes: a second-order perturbative treatment was proposed by de Loth et al.[7] for biradicals, giving reasonable agreement with experiment for a number of bridged copper dimers. Noodleman's broken symmetry approach[8] was also applied to this family.

Among copper dimers, μ-oxalato Cu(II) binuclear complexes constitute a very rich family since there is a wide variety of compounds with different external ligands.[4,9−13] Most frequently, copper is pentacoordinated,[9−13] in complexes with $[L_3Cu(\mu\text{-}C_2O_4)CuL_3]^{2+}$ generic formula, where L_3 stands for external ligands, from three monodentate to a single tridentate ligand, usually coordinated by nitrogen or oxygen centers. In parallel with the volume of experimental information, μ-oxalato Cu(II) binuclear complexes have also been favored by the attention of theoreticians at different levels of theory.[5,14−16] A particular subset of the synthesized compounds belonging to this family involves a variety of aminic ligands. Several complexes of this type have been crystallographically and magnetically characterized.[9−12]

To fit the experimental susceptibility versus temperature data, the spin interaction is usually described through the phenomenological Heisenberg Hamiltonian:

$$\hat{H} = -2J\hat{S}_1\hat{S}_2 \tag{1}$$

where $\hat{S}_1$ and $\hat{S}_2$ are the local spin operators and J is the exchange coupling constant. The energy difference between two states of S and $S-1$ total spin is given by

$$E(S-1) - E(S) = 2JS \tag{2}$$

In this formulation, a negative value of the coupling constant indicates antiferromagnetic coupling, usually interpreted through Anderson's[17] superexchange mechanism. Other terms such as biquadratic exchange terms may be added to (1) to obtain better data fitting. Only when the contribution of these additional terms becomes important may the energy transitions deviate from expression (2).

The theoretical estimation of J consists thus in evaluating the energy difference between states of different multiplicity. The magnetic interaction in copper (d^9) binuclear complexes leads to two possible states, a triplet and a singlet, and thus

$$E(\mathrm{S}) - E(\mathrm{T}) = 2J \tag{3}$$

where S and T stands for the singlet and the triplet states, respectively. The purpose of the present work is to give an accurate evaluation of the exchange coupling constant versus the structural changes in $[L_3Cu(\mu\text{-}C_2O_4)CuL_3]^{2+}$, where L_3 are N-coordinated ligands, by means of the difference-dedicated configuration interaction (DDCI2) method.[18]

[†] Universitat Rovira i Virgili.
[‡] Present address: Laboratoire de Chimie Quantique, UMR 7551, Université Louis Pasteur, 4 rue Blaise Pascal, Strasbourg, France.
[§] Universitat de Barcelona.

10.1021/jp001908e CCC: $19.00
Published on Web 10/13/2000

On the basis of the second-order perturbative treatment by de Loth et al.,[7] in previous papers,[18−22] we presented a variational method especially conceived to determine energy transitions in these and more complex magnetic systems, referred by the acronym DDCI2 since it is the version specifically suited for magnetic systems of the more general difference-dedicated configuration interaction method (DDCI).[23] The method starts by giving a simple zeroth-order description of the energy difference. Differential second-order contributions are then added variationally. DDCI2 has been applied successfully to organic biradicals,[20,24] to transition metal binuclear complexes with different types of bridging ligands,[18,21,22] and to various families of ionic solids.[25−27] A summary of the DDCI2 method is given in section 3.

In this paper, the DDCI2 method has been applied to the model (μ-oxalato)bis[triamminecopper(II)] cation, $[(NH_3)_6Cu_2(\mu\text{-}C_2O_4)]^{2+}$, to analyze the structural dependence of the coupling constant found in a series of $[L_3Cu(\mu\text{-}C_2O_4)CuL_3]^{2+}$complexes, in which the nitrogen-coordinated ligands have been substituted by NH_3. Two types of geometrical structures have been considered: (i) three C_{2h} geometries that correspond to limit coordination types of copper as will be discussed in terms of orbital analysis in section 2 and (ii) four centrosymmetric geometries for which the structural parameters have been taken from the crystallographic data of $[(Et_5dien)_2Cu_2(\mu\text{-}C_2O_4)](BPh_4)_2$ (**1**)[9,11] (Et_5dien = 1,1,4,7,7-pentaethyldiethylenetriamine), $[(Et_5dien)_2Cu_2(\mu\text{-}C_2O_4)](PF_6)_2$ (**2**)[9,11] and $[(tmen,2\text{-}MeIm)_2Cu_2(\mu\text{-}C_2O_4)](PF_6)_2$ (**3**)[12] (tmen = *N*,*N*,*N*′,*N*′-tetramethylethylenediamine and 2-MeIm = 2-methylimidazole), and $[(dien)_2Cu_2(\mu\text{-}C_2O_4)](ClO_4)_2$ (**4**)[10] (dien = diethylenetriamine). The results are presented in section 4.

Finally, the effect of external ligands has been studied by unrestricted Hartree−Fock (UHF) and density functional theory (DFT) calculations within Noodleman's broken symmetry approach[8] on the real $[(Et_5dien)_2Cu_2(\mu\text{-}C_2O_4)]^{2+}$ complex and on the $[(NH_3)_6Cu_2(\mu\text{-}C_2O_4)]^{2+}$ model in the same geometry. It is worth pointing out that the use of a single unrestricted Slater (or Kohn−Sham) determinant does not permit us to obtain pure spin eigenfunctions, instead symmetry-adapted high spin (HS) and broken symmetry low spin states (BS) are obtained. The former is a reasonable approximation to the real triplet state (T) whereas the later corresponds to a fake state whose energy is midway between the singlet and triplet.[28,29] In this approach, the coupling constant for a biradical has to be evaluated through the expression

$$J = \frac{E(\mathrm{BS}) - E(\mathrm{T})}{1 + S_{\mathrm{ab}}{}^2} \tag{4}$$

with E(BS) and E(T) the energies of the unrestricted spin broken symmetry low-spin state and of the triplet, respectively, and S_{ab} the overlap between the magnetic orbitals. Since the alpha and beta spin orbitals are nearly orthogonal, the equivalent of eq 4 is

$$E(\mathrm{S}) - E(\mathrm{T}) = 2\{E(\mathrm{BS}) - E(\mathrm{T})\} = 2J \tag{5}$$

where E(S) is the energy of the true singlet or

$$E(\mathrm{BS}) - E(\mathrm{T}) = J \tag{6}$$

The broken symmetry approach has been extensively applied to magnetic systems with considerable success[16,30] although the choice of the exchange-correlation functional is a delicate point[28] and results have to be interpreted with caution.[29] The DFT analysis of the effect of modeling the external ligands is discussed in section 5.

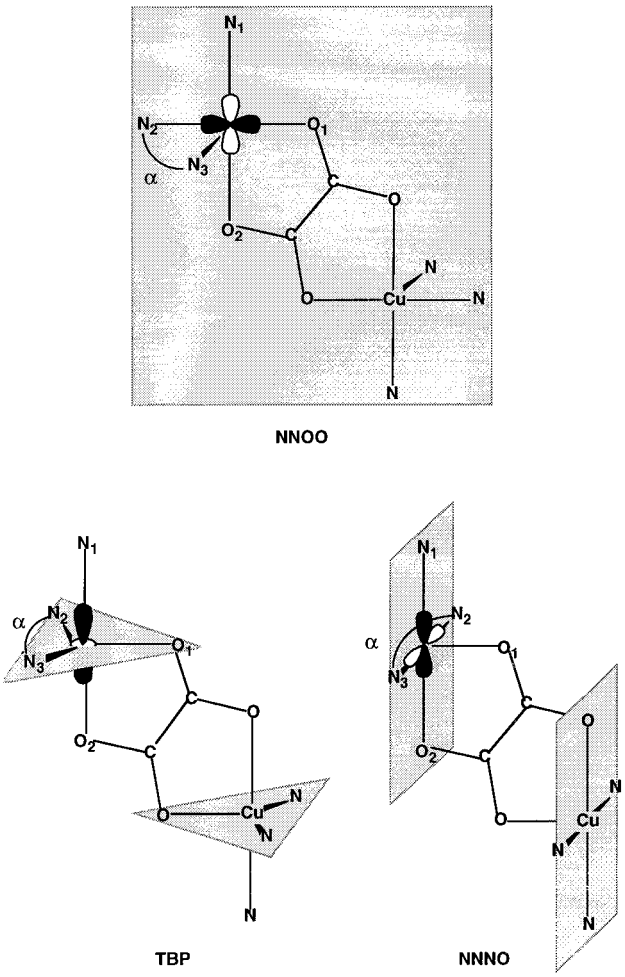

Figure 1. Schematic representation of $[(NH_3)_6Cu_2(\mu\text{-}C_2O_4)]^{2+}$ structure, in the three limit coordinations: NNOO, TBP and NNNO.

2. Orbital Analysis of the Magneto−Structural Dependence

The structures of pentacoordinated μ-oxalato copper(II) complexes described in the literature are intermediate between three limit geometries, depending on the external ligands, as represented in Figure 1:

(a) a trigonal bipyramid (TBP), in which the trigonal plane is defined by two nitrogen atoms of the external ligands and one oxygen atom of the oxalato group, the apical positions being occupied by the remaining oxygen of $C_2O_4^{2-}$ and the nitrogen of the third external ligand;

(b) a square basis pyramid (NNOO), in which the basal plane is defined by both oxygen atoms of the oxalato group and two nitrogen atoms of the external ligands, the axial position being occupied by the remaining nitrogen external ligand. Both cis and trans configurations are possible. Since the trans configuration is frequent with H_2O ligands in the axial position, this is the only case considered here.

(c) a square basis pyramid (NNNO), in which the basal plane is defined by the three nitrogen atoms of the external ligands and one oxygen atom of the oxalato group, the axial position being occupied by the remaining oxalato oxygen.

Many previous works have shown that changes in the external ligands and in the counterion lead to changes in the geometry of the copper coordination affecting the exchange interac-

tion.[1b,9−13,16] Single electron considerations give a simple rationale to the trend of variation of the exchange interaction: Figure 1 shows for the three cases (TBP, NNNO, and NNOO) the metal orbital interacting with the appropriate symmetry-adapted lone-pair orbitals of the oxalato group.

In the NNOO structure, the magnetic orbitals can be described by $d_{x^2-y^2}$ symmetric and antisymmetric combinations interacting with the oxalato bridge. The coplanar topology maximizes the overlap between the metal and the oxalato group orbitals. The smallest interaction occurs in the NNNO structure in which the magnetic orbitals can also be described by $d_{x^2-y^2}$ combinations parallel between them but perpendicular to oxalato bridge. Finally, in the TBP structure, the magnetic orbitals can be described by symmetric and antisymmetric combinations of d_{z^2} type orbitals with an intermediate overlap with the oxalato bridge.

With this qualitative description of the magnetic orbitals and their overlap with the appropriate oxalato group orbitals, the magnitude of the exchange coupling constant is expected to decrease following the trend:

$$|J_{\mathrm{NNOO}}| > |J_{\mathrm{TBP}}| > |J_{\mathrm{NNNO}}|$$

When trying to synthesize the most important variations between the three geometries with a small number of structural parameters, it is easy to see that a single parameter, the angle between two nitrogen atoms in the plane orthogonal to the oxalato bridge, the α angle defined in Figure 1, summarizes these changes, since $\alpha = 90°$ in NNOO, 120° in TBP, and 180° in NNNO. Upon increasing α, the geometry is induced to change from the NNOO square basis pyramid to the TBP structure and finally to the NNNO one. In conclusion, as α increases, $|J|$ decreases. This trend will be confirmed, for the models as well as the real complexes, by the present results as will be shown in section 4.

3. CI Method To Evaluate the Exchange Constant

3.1. DDCI2 Method. The DDCI2 method, the reduced version of DDCI specifically designed for magnetic systems, is based on the early perturbative work by De Loth et al.[7] It was first derived to evaluate singlet−triplet gaps in biradicals[18a] and was later generalized for systems with a higher number of unpaired electrons.[19] The DDCI2 method is based on the definition of a minimal model space *S*, defined from the *n* singly occupied "magnetic orbitals". This model space is generated by the neutral determinants, in the valence bond (VB) terminology, i.e., the subspace of the complete active space (CAS) generated from the *n* localized orbitals and the *n* electrons defined with determinants built from different spatial orbitals. For biradicals such as Cu(II) dimers, in which the copper configuration is d^9, the space would be formally generated by the neutral determinants $|a\bar{b}\rangle$ and $|b\bar{a}\rangle$ built from the d singly occupied orbitals, a and b, i.e., $Cu(d^9)-Cu(d^9)$ determinants.

In the framework of the quasi-degenerate perturbation theory, it has been demonstrated[18a] that of all the double excitations that contribute to the second-order development of the corresponding effective Hamiltonian, only those with at most two inactive orbitals (occupied or virtual) are significant for the spectrum. The model space and these double excitations that contribute to the energy differences define the DDCI2 space, which is a subspace of the CAS single double configuration interaction (CAS*SDCI). To include higher orders of perturbation, the DDCI2 space is then treated variationally and the value of the exchange coupling constant is determined from the difference between two roots through eq 2. The physical effects that are considered in the DDCI2 treatment include all the contributions up to second order as discussed by de Loth et al.: potential exchange, kinetic exchange, dynamic spin polarization and charge transfer. The variational treatment, however, introduces higher-order effects which include the contributions enabling the relaxation of the ionic determinants $|a\bar{a}\rangle$ and $|b\bar{b}\rangle$ (i.e., $Cu(d^{10})-Cu(d^8)$ determinants), in the VB terminology, that appear only at the fourth order. This last effect is important because the magnetic orbitals are well adapted to describe the neutral determinants, in which they are singly occupied, but not the ionic ones, whose energy is largely overestimated.

Complementary determinants are added to ensure that the wave functions are eigenfunctions of $\hat{S}^2$ and space symmetry is also taken into account. Unitary transformations of the active MOs keep the wave function invariant and the magnetic orbitals are only needed for a formal purpose because the selection criterion is based on a VB formalism. The DDCI2 space thus includes (1) the CAS generated from the *n* unpaired electrons and the *n* active symmetry-adapted MOs, which are essentially bonding and antibonding combinations of d atomic orbitals centered on the magnetic center with small contributions of the neighbor ligands, i.e., a CAS (2,2) in the present system, and (2) all singles and doubles on the CAS involving at most two inactive orbitals, either holes or particles. The main characteristics of the DDCI2 method may be summarized in four points: (i) it is a strictly variational method and for this reason (ii) it is an uncontracted method which allows the external correlation to modify the coefficients of the CAS; (iii) the DDCI2 matrix is invariant under rotations of the molecular orbitals (MOs) in the active, doubly occupied or virtual subsets and therefore the method takes advantage of working with symmetry adapted MOs; and (iv) the number of determinants in the DDCI2 space is proportional to the square of the dimension of the MO set, instead of to the fourth power as it is in a CAS*SDCI calculation.

3.2. Role of the Relaxation of the Bridge-Ligand to Metal Charge-Transfer Configurations. Recently, Calzado et al.[31] have shown that in systems in which important charge transfer from the bridging ligand (BL) to the metal (M) occurs, DDCI2 systematically underestimates the antiferromagnetic coupling. As is well-known, in the Anderson mechanism the mixing of the ionic forms $|a\bar{a}\rangle$ and $|b\bar{b}\rangle$ with the singlet state is responsible for the antiferromagnetic coupling. DDCI2 includes this interaction as well as the indirect superexchange mechanism through BL → M charge transfer. But these authors also observe that the stability of the singlet increases and the weight of the charge-transfer configurations is enhanced when increasing the DDCI2 list of determinants with their instantaneous repolarization (determinants with two inactive holes and one inactive particle, not included in the original list, i.e., single excitations on BL → M charge transfer, SLMCT, configurations). The interpretation of this effect is given in the VB context, since the inclusion of SLMCT contributions allows a better instantaneous relaxation of the ionic forms, $|a\bar{a}\rangle$ and $|b\bar{b}\rangle$, whose weight is consequently increased in the singlet state wave function. The energy of the singlet is stabilized in this way. The CI space has to be enlarged with these determinants and the resulting space will be called hereafter DDCI2+SLMCT. A second alternative[31b,c] is to perform a complete DDCI[23] calculation, which includes all doubles with up to three inactive determinants and among them the significant contributions here discussed. Calzado et al.[31a] have shown the additional determinants of DDCI not to be significant for the magnetic exchange coupling. Since the price

TABLE 1: Most Significant Bond Lengths (in Ångstrom) Used for the Different Models, NNOO, TBP, and NNNO[a]

	model		
bond length	NNOO	TBP	NNNO
Cu−Cu	5.495	5.410	5.433
$Cu-O_1$	2.122	2.074	1.962
$Cu-O_2$	2.122	2.074	2.235
C−C	1.570	1.527	1.549
$Cu-N_1$	2.163	2.011	1.983
$Cu-N_2$	2.163	2.139	1.993
$Cu-N_3$	2.042	2.139	1.993

[a] See Figure 1 for details.

of a DDCI calculation is to enlarge the CI space considerably (the complete DDCI space dimension is proportional to the third power of the basis set dimension), the generation of the charge transfer determinants has been implemented in the DDCI/DDCI2 code. As will be shown below, the difference in the results arising from the repolarization of the charge-transfer contributions with the oxalato bridging ligand is substantial.

3.3. Molecular Orbital Choice. Since the results may be dependent on the molecular orbitals (MOs) used in the CI step, an iterative improvement in the active orbitals has been proposed[23c,d] to avoid this difficulty. In this iterative technique (IDDCI) an average density matrix $\bar{\mathbf{R}}$ is obtained by adding the density matrices of the singlet ($\mathbf{R}_S$) and of the triplet states ($\mathbf{R}_T$): $\bar{\mathbf{R}} = {}^1/_2(\mathbf{R}_S + \mathbf{R}_T)$. Average natural orbitals adapted to both states are obtained by diagonalizing $\bar{\mathbf{R}}$. The method is completely general and does not depend on the structure of the CI space used in the calculation. We have used this procedure, iterating the natural orbitals obtained after the DDCI2+SLMCT calculation.

4. DDCI2 Exchange Coupling Constant in $[(NH_3)_6Cu_2(\mu\text{-}C_2O_4)]^{2+}$

4.1. Computational Details. Two series of calculations have been performed on the $[(NH_3)_6Cu_2(\mu\text{-}C_2O_4)]^{2+}$ complex, the first one using the limit geometries, corresponding to the highly symmetric NNOO, TBP, and NNNO structures, all belonging to the C_{2h} point group, and the second one using the structural parameters of four centrosymmetric compounds that have been crystallographically and magnetically characterized. The geometries of the NNOO, TPB, and NNNO models have been generated from the crystallographic data of the characterized complexes, by increasing the symmetry. Table 1 gives the most relevant parameters. In all DDCI2 calculations, NH_3 ligands have been used to model the external ligands since the complexes studied have in general saturated amine-type ligands and the external ligands have little influence on the J value, provided that the coordination of the metal and the electronegativity are preserved. A discussion of this point is given in section 5.

All electron calculations on $[(NH_3)_6Cu_2(\mu\text{-}C_2O_4)]^{2+}$ have been performed by using ANO (atomic natural orbitals) basis sets with a (6s5p3d1f) contraction for Cu and (3s2p) for the second row atoms. The external ligands are expected to play a small role in the magnetic coupling because of the local character of the interaction. If a DZ basis set is used for NH_3 ligands, the complete DDCI2 calculation is not possible because the size of the two electron molecular integrals file exceeds the storage capabilities of our equipment. The truncation of the MO set is always a delicate problem since in general the energy ordering is not a good criterion to evaluate the role of the orbitals in the correlation energy. An alternative giving a rational way for the truncation is to use projection techniques to concentrate the MOs playing a small role in the correlation and then to freeze them at the integral transformation level. In the $[(NH_3)_6Cu_2(\mu\text{-}C_2O_4)]^{2+}$ complex, the doubly occupied MOs have been projected onto the occupied MOs of the $(NH_3)_6$ fragment as a whole obtained from a separate calculation. Several tests have been performed on the models with a small basis set (STO-6G) for the NH_3 groups to analyze the effect on the exchange coupling constant of truncating the MO set after the localization procedure. The results reported in Table 2 show that the effect on J is small, less than 4 cm^{-1}. Within a comparable accuracy, the reduction of the two-electron integrals file size and of the CI spaces dimension are quite significant: the size of the integrals file decreases from 300 to 100 Mb and the dimension of the CI space from 21000 (DDCI2) and 100000 (DDCI2+TC) to 13000 and 60000, respectively. This technique makes the calculation feasible when larger basis sets are used.

TABLE 2: Effect on J (cm^{-1}) of Freezing the MO Set after Localization of the Orbitals of the $(NH_3)_6$ Fragment at the DDCI2 and DDCI2+SLMCT Levels, for Two Models, TBP and NNNO, with a STO-6G Basis Set for the NH_3 Ligands[a]

	complete MO set		truncated	
model	J_{DDCI2}	$J_{DDCI2+SLMCT}$[b]	J_{DDCI2}	$J_{DDCI2+SLMCT}$[b]
TBP	−8.2	−49.7	−6.0	−53.2
NNNO	+0.2	+1.4	+1.0	+2.2

[a] Starting MOs obtained from a CASSCF (10,10) calculation. [b] Iterated MOs

TABLE 3: Exchange Coupling Constant, J (cm^{-1}), of TBP, as a Function of the Starting MOs

MOs	DDCI2	DDCI2+SLMCT	DDCI2+SLMCT (IDDCI)
CASSCF (2,2)	−6.4	−35.8	−38.3
CASSCF (10,10)	−6.9	−49.1	−71.8

In contrast to previous studies using DDCI2, the choice of the starting MOs has proven to be crucial for the quality of the results, since the oxalato MOs are very sensitive to the CASSCF procedure. The MOs implicated in the charge transfer process are the oxygen lone pairs and copper d orbitals. The MOs quality when starting the IDDCI optimization is very important for a fast convergence. To evaluate the size of the active space at the CASSCF level to get meaningful MOs, several tests have been performed adding or not the oxalato lone pairs and their correlation in the active space. This enlarged CAS (10,10) includes then: the bonding and antibonding d combinations as discussed previously included in the CAS(2,2), the four symmetry compatible combinations of the sigma oxalato-lone pairs and the four oxalato virtual orbitals of the same irreducible representations. Nevertheless, it must be pointed out that the DDCI2 space is in all cases selected from two active orbitals only, the bonding and antibonding d combinations obtained when the CASSCF(10,10) triplet is converged. Table 3 shows the DDCI2 and DDCI2+SLMCT results for the TBP model. The large increase of J suggests that a CAS (10,10) must be used at this level.

All the calculations until the transformation to the molecular two-electron integrals have been performed by using the MOLCAS 4.1 package.[32] The DDCI-SCIEL[33,34] programs have been used in the CI calculations. In all cases, the lowest triplet and singlet have been calculated, and J has been evaluated by eq 3: $E(S) - E(T) = 2J$.

4.2. Extraction of the Exchange Coupling Constant. A set of calculations on the magneto-structural dependence have been performed on the three model structures of the $[(NH_3)_6Cu_2(\mu\text{-}C_2O_4)]^{2+}$ complex indicated in Figure 1: NNOO, TBP, and

TABLE 4: Exchange Coupling Constants, J (cm^{-1}), of Different $[Cu_2(ox)(NH_3)_6]^{2+}$ Structures[a]

complex structure	coordination	a	J_{DDCI2}	$J_{DDCI2+SLMCT}$	J_{exp}
model	NNOO	90	−16.9	−138.6	
model	TBP	120	−6.95	−71.8	
model	NNNO	180	+0.1	−1.8	
M1	∼TBP	130	−9.7	−38.1	−37.4[b]
M2	intermediate	153	−2.1	−13.1	−9.6[b]
M3	intermediate	153	−1.3	−7.4	−7[c]
M4	∼NNNO	160	0.0	−1.7	< |−0.5|[d]

[a] The original geometry, the type of coordination and the N_2CuN_3 bond angle, α (deg), are indicated for each structure. The geometries **M1**, **M2**, **M3**, and **M4** of the complex correspond to the crystallographic data of: $[(Et_5dien)_2Cu_2(\mu\text{-}C_2O_4)](BPh_4)_2$ (**1**), $[(Et_5dien)_2Cu_2(\mu\text{-}C_2O_4)](PF_6)_2$ (**2**), $[(tmen,2\text{-}MeIm)_2Cu_2(\mu\text{-}C_2O_4)](PF_6)_2$ (**3**), and $[(dien)_2Cu_2(\mu\text{-}C_2O_4)](ClO_4)_2$ (**4**), respectively. [b] References 9 and 11. [c] Reference 12. [d] Reference 10.

NNNO. All these structures belong to C_{2h} symmetry point groups. According to the above qualitative analysis, the active MOs are symmetric and antisymmetric combinations of the appropriate d orbital of the copper centers with contribution of the symmetry adapted oxalato lone pairs. Thus, the active MOs belong to the a_g and b_u irreducible representations (IR) for TBP and NNNO and to a_u and b_g IR for NNOO. The singlet and triplet states are thus ^1A_g and ^3B_u for the three models.

The size of the DDCI2 space is around 20000 determinants in all cases. The results are reported in Table 4. One main feature emerges from the table: the calculated exchange coupling constant follows the expected trend. According to the definition of α (see Figure 1), the antiferromagnetic coupling decreases with increasing α, i.e. from NNOO (α = 90°) to NNNO (α = 180°). The last coupling is found to be 0.1 cm^{-1}, at the limit of the calculation precision, and both states must be considered degenerate.

In a second step, four geometries corresponding to experimentally described complexes have been used in the calculations. The geometrical parameters of the oxalato bridge and the position of the external ligands have been taken from the crystallographic data of a structure very close to TBP, $[(Et_5dien)_2Cu_2(\mu\text{-}C_2O_4)](BPh_4)_2$ (Et_5dien = 1,1,4,7,7-pentaethyldiethylenetriamine) (**1**), with α = 130°, and three intermediate structures between TBP and NNNO structures, $[(Et_5dien)_2Cu_2(\mu\text{-}C_2O_4)](PF_6)_2$ (**2**), $[(tmen,2\text{-}MeIm)_2Cu_2(\mu\text{-}C_2O_4)](PF_6)_2$ (tmen = *N*,*N*,*N*′,*N*′-tetramethylethylenediamine, 2-MeIm = 2-methylimidazole) (**3**), both with α = 153°, and $[(dien)_2Cu_2(\mu\text{-}C_2O_4)](ClO_4)_2$ (dien = diethylenetriamine) (**4**), with α = 160°. A plot of the $[(Et_5dien)_2Cu_2(\mu\text{-}C_2O_4)]^{2+}$ complex structure in compound **1** is given in Figure 2. The corresponding $[(NH_3)_6Cu_2(\mu\text{-}C_2O_4)]^{2+}$ models will be referred hereafter as **M1**, **M2**, **M3**, and **M4**, respectively.

All the structures are centrosymmetric and belong to C_i point group. The active orbitals belong to the a_g and a_u IR. The dimension of the ^1A_g and ^3A_u DDCI2 spaces is around 27000 determinants. The results reported in Table 4 show the same trend as that of the models: the largest coupling corresponds to the smallest α angle. When compared with the experimental data, the sign and the trend of the coupling are correctly reproduced, but all the constants are strongly underestimated. As mentioned before, this is the same trend as observed in the calculated exchange constant in ionic solids with important BL → M charge-transfer contributions to the wave function. The effect of the polarization on the charge transfer determinants on the C_{2h} models is dramatic: as shown in Table 4, DDCI2+SLMCT multiplies the value of the exchange coupling constant by a factor of around seven. The effect on **M1**−**M4** is also very significant, since the addition of these determinants increases the value of the coupling constant by a similar factor. When comparing these results to experiment, the agreement is excellent. The addition of complementary determinants only enlarges the DDCI2+SLMCT spaces by a factor of around 4 compared to the DDCI2 ones, so that the method reaches a very high degree of accuracy but remains economic.

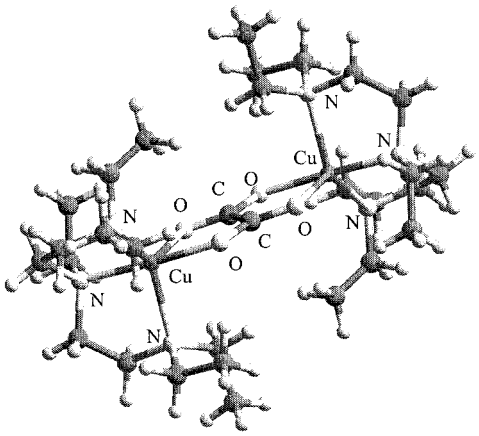

Figure 2. Structure of $[(Et_5dien)_2Cu_2(\mu\text{-}C_2O_4)]^{2+}$.

5. Role of the External Ligands

The role of the external ligands is a matter of discussion[16,35] although it is in general assumed that, if the type of coordination and the electronegativity of the ligands are preserved, they have minor influence on the exchange coupling constant. From one-electron considerations[35] as well as from DFT calculations,[16] it has been concluded that the larger σ donor character of the ligands gives rise to stronger antiferromagnetic compared with NH_3 ligands. Since the external ligands of the complexes analyzed here are tertiary amines, and since it is assumed that the σ donor character of a tertiary amine is larger than the ammonia one, the expected result of the comparison is that the calculated J values presented in the precedent section are slightly underestimated. Higher values are expected if the complete calculation was possible at the DDCI level. These calculations are not feasible in the real complexes discussed here, but this analysis can be carried out by means of DFT based methods within the broken symmetry approach, as discussed above. To obtain an estimate of the importance of the error of the DDCI values induced by the modeling, DFT calculations have been performed on **1** chosen as a representative system.

5.1. Details of the DFT Calculations. Two sets of DFT calculations have been performed. The first set was carried out on the **M1** model used in the DDCI calculations described in the preceding section, in which the external ligands are substituted by NH_3 groups. In the second set of calculations the real ligands of compound **1** (see Figure 2) at the experimental geometry have been considered. For comparison, two different functionals have been used: the commonly used B3LYP[36] and BF:LYP defined by Martin and Illas.[30] Both functionals are of the hybrid type and differ on the amount of Hartree−Fock exchange introduced but use the same definition of the correlation functional. B3LYP uses ∼20% Fock exchange whereas BF:LYP uses a 50% mixture of Fock and Becke's gradient-corrected exchange functional. Two basis sets have been used in the DFT calculations depending on whether NH_3 or real ligands are considered. The quality of these basis sets differs only in the most external atoms. For the complex with NH_3 ligands, **M1**,

TABLE 5: Effect of Modeling the External Ligands on the Exchange Coupling Constant J (cm^{-1}) of $[(Et_5dien)_2Cu_2(\mu\text{-}C_2O_4)](BPh_4)_2$ (1) at the DFT Level, Using the Broken Symmetry Approach (BS)

	broken symmetry				
complex	UHF	BF:LYP	B3LYP	$J_{DDCI2+SLMCT}$	J_{exp}
$[(NH_3)_6Cu_2(\mu-C_2O_4)]^{2+}$, **M1**	−5.3	−28.1	−148.6	−38.1	
$[(Et_5dien)_2Cu_2(\mu-C_2O_4)]^{2+}$, **1**	−4.7	−21.6	−89.5		−37.4[a]

[a] Reference 9 and 11.

TABLE 6: Spin Density and Mulliken Charges on $[L_2Cu_2(\mu\text{-}C_2O_4)]^{2+}$, with L = $(NH_3)_3$, Et_5dien[a]

		spin density				Mulliken charges			
complex	method	Cu	O_1	O_2	N[b]	Cu	O_1	O_2	N
$[(NH_3)_6Cu_2(\mu\text{-}C_2O_4)]^{2+}$, **M1**	UHF	0.93	0.02	0.01	0.06	1.56	−0.85	−0.76	−0.92
	BF:LYP	0.84	0.05	0.01	0.12	1.37	−0.71	−0.64	−0.85
	B3LYP	0.70	0.09	0.02	0.18	1.21	−0.61	−0.55	−0.79
$[(Et_5dien)_2Cu_2(\mu\text{-}C_2O_4)]^{2+}$, **1**	UHF	0.93	0.02	0.01	0.07	1.60	−0.84	−0.76	−1.07
	BF:LYP	0.82	0.04	0.01	0.14	1.37	−0.70	−0.63	−0.87
	B3LYP	0.66	0.07	0.01	0.24	1.18	−0.60	−0.55	−0.75

[a] The four oxygen atoms in the oxolato bridge are two by two different. [b] Sum over the three N atoms.

we have used a 6-3111+g basis augmented with an f function (exponent = 0.5203) for Cu and 6-31G** for C, N, O and H. For the complex with the real ligands the basis is the same except on C and H atoms of the most external ligands described by means of a 6-31G basis. All DFT calculations have been carried out with the Gaussian98 package of programs.[37]

5.2. Results. From the summary of results presented in Table 5 several points emerge. The first is that the results obtained with different exchange-correlation functionals, $E_{XC}[\rho]$, corroborate the strong dependence of the magnetic coupling constant J with respect to the choice of $E_{XC}[\rho]$. In particular, J increases monotonically with the increase of DFT exchange in agreement with results reported for a variety of ionic solids.[30] This is a well-known effect that arises from the tendency of LDA, and even GGA, to underestimate the HOMO−LUMO gap, thus favoring closed shell metallic systems above the proper biradical character of these compounds. From the comparison with full CI (FCI) calculations on models[28] it has been shown that B3LYP overestimates the antiferromagnetic coupling when taking into account the small overlap between the magnetic orbitals in eq 6. This trend is related to a strong delocalization of the spin density. Polarized neutron diffraction experiments on oxamato and oxamido bridged Mn(II)-Cu(II) compounds[38] are in line with the observation that DFT predicts too low spin densities on the metal. According to this evidence, it is expected that by increasing the Hartree−Fock character in $E_{XC}[\rho]$, a better description of the spin density is obtained. This trend is confirmed by the spin densities reported in Table 6. Since the spin densities and the Mulliken charges are virtually identical for both the triplet and the broken symmetry states only the BS ones are reported.

A second important feature is the strong dependence of the role of the external ligands on the particular choice of $E_{XC}[\rho]$. Substituting the real ligands by NH_3 molecules has a 13% effect on the UHF calculated J which becomes 26% for the BF:LYP method and reaches 66% for the B3LYP method.[39] This dependence with respect to $E_{XC}[\rho]$ can also be related to delocalization, since Table 6 shows that the difference of the spin density between the model and the real complex increases from UHF to B3LYP calculations, which induce a larger delocalization of the spin density toward the external ligands. The bridge atom spin densities are not significantly changed. Not easily understood, however, is the trend induced by the ligands. As argued above, the donor character of the real ligands suggests an increase of J. However, results in Table 5 do not support this apparently too simple reasoning. The changes in the net charges on copper and the bridging-ligand obtained from a Mulliken population analysis do not bring much additional information, since no noticeable changes appear between the model and the real complex. The decrease in J when NH_3 are substituted by real ligands is accompanied by a decrease in the spin density of the magnetic centers without any noticeable change in the charge distribution within a given choice of $E_{XC}[\rho]$, as shown in Table 6. Hence, it becomes difficult to decide whether the significant effect of the ligands predicted by the DFT models has physical significance or responds to the tendency of these methods to overestimate delocalization effects. Since the BF:LYP value on the real complex seems to be in a better coincidence with the experimental one, and since the coupling constant predicted by this method on the model is in reasonable agreement with DDCI results, the magnitude of the effect of the ligands on J found by this method, around 6 cm^{-1}, seems to be more reliable. Furthermore, from comparisons[28,40] with exact spin densities on some models shows that UHF gives the smallest deviation and, among hybrid DFT methods, B3LYP the largest. As shown in Table 5, at the UHF level, the effect is really small. This indicates that the values calculated at the DDCI level would not be significantly changed if the effect of the external ligands could be included at this refined level of theory.

6. Conclusions

The results show that the DDCI2 method, which has previously been proven to give estimations of the exchange coupling constant in good agreement with the experiment on a variety of systems, systematically underestimates the coupling in μ-oxalato-Cu(II) binuclear complexes. Nevertheless, by enlarging the CI space only with those configurations that allow the instantaneous relaxation of the configurations connected to the charge transfer excitations from the bridging ligand to the metal, excellent results are reached. Not only do the DDCI2+SLMCT results show the expected trend for the NNOO, TBP, and NNNO models but also the magnitude of the exchange coupling is quantitatively reproduced for four $[(NH_3)_6Cu_2(\mu\text{-}C_2O_4)]^{2+}$ model complexes reproducing the experimental structure. By introducing only this strictly necessary part of the correlation in a DDCI2+SLMCT calculation, the amount of computation requirements is limited since the dimension of the CI space remains small. The localization technique used before freezing the molecular orbitals of the

external ligands allows a considerable reduction of the storage requirements and is proven to be quite efficient since the deviation from the *J* values obtained in from the full calculation ones is very small.

The effect of the external ligands is found to depend largely on the method used, although a reasonable estimate is that the effect on *J* is not larger than 8−10 cm^{-1} in the most antiferromagnetic complex here presented, hence supporting the use of simple models and accurate methods, in particular the DDCI2+SLMCT as described above. However, a point that remains to be properly understood is the reason the effect predicted by DFT methods of substituting the tertiary amine-type external ligands by NH_3 is to increase the antiferromagnetic character in contradiction with the result expected from the smaller σ-donor character of NH_3.

Acknowledgment. We are indebted to the DGICYT of the Ministerio de Educación y Ciencia of Spain (projects PB98-1216-CO2-01 and PB98-1216-CO2-02) and to the CIRIT of the Generalitat de Catalunya (grants SGR99-182 and SGR99-40) for financial support. C.deG. thanks the European Commission for the Marie Curie research training grant FMBICT983279. N.B. is indebted to the European Commission for a postdoctoral fellowship (TMR network contract ERBFMRX-CT96-0079, Quantum Chemistry of Excited States). We acknowledge J. P. Malrieu and C. J. Calzado for fruitful discussions and comments.

References and Notes

(1) (a) Bencini, A.; Gatteschi, D.; Zanchini, C. *Inorg. Chem*. **1985**, *24*, 704. (b) Willett, R. D. In *Magneto Structural Correlations in Exchange Coupled Systems*; Willett, R. D.; Gatteschi, D.; Kahn, O., Eds.; NATO Advanced Studies Series. C, Vol. 140; Reidel: Dordrecht, 1985; p 389.

(2) (a) Comarmond, J.; Pluméré, P.; Lehn, J.-M.; Agnus, Y.; Louis, R.; Weiss, R.; Kahn, O.; Morgestern-Badarau, I. *J. Am. Chem. Soc.* **1982**, *104*, 6330; (b) Kahn, O.; Sikorav, S.; Gouteron, J.; Jeannin, S.; Jeannin, Y. *Inorg. Chem*. **1983**, *22*, 2883.

(3) Hatfield, W. E. In *Magneto Structural Correlations in Exchange Coupled Systems*; Willett, R. D.; Gatteschi, D.; Kahn, O., Eds.; NATO Advanced Studies Series. C, Vol. 140; Reidel: Dordrecht, 1985; p 555.

(4) Glerup, J.; Goodson, P. A.; Hodgson, D. J.; Michelsen, K. *Inorg. Chem*. **1995**, *34*, 6255.

(5) Hay, P. J.; Thibeault, J. C.; Hoffmann, R. *J. Am. Chem. Soc.* **1975**, *97*, 7, 4884.

(6) Kahn, O. *Angew. Chem., Int. Ed. Engl*. **1985**, *24*, 834 and references therein.

(7) (a) De Loth, P.; Cassoux, P.; Daudey, J. P.; Malrieu, J. P. *J. Am. Chem. Soc*. **1981**, *103*, 4007. (b) Charlot, M. F.; Verdaguer, M.; Journaux, Y.; De Loth, P.; Daudey, J. P. *Inorg. Chem.* **1984**, *23*, 3802. (c) De Loth, P.; Daudey, J. P.; Astheimer, H.; Walz, L.; Haase, W. *J. Chem. Phys.* **1985**, *82*, 5048. (d) De Loth, P.; Karafiloglou, P.; Daudey, J. P.; Kahn, O. *J. Am. Chem. Soc.* **1988**, *110*, 5676. (e) Daudey, J. P.; De Loth, Ph.; Malrieu, J. P. In *Magneto Structural Correlations in Exchange Coupled Systems*; Willett, R. D.; Gatteschi, D.; Kahn, O., Eds.; NATO Advanced Studies Series. C, Vol. 140; Reidel: Dordrecht, 1985; p 87.

(8) Noodleman, L. *J. Chem. Phys.* **1981**, *74*, 5737.

(9) Hall, G. R.; Duggan, M.; Hendrickson, D. N. *Inorg. Chem*. **1975**, *14*, 1956.

(10) Felthouse, T. R.; Laskowski, E. J.; Biekksza, D. S.; Hendrickson, D. N. *J. Chem. Soc. Chem. Commun.* **1977**, 777.

(11) Felthouse, T. R.; Laskowski, E. J.; Hendrickson, D. N. *Inorg. Chem.* **1977**, *16*, 1077.

(12) Julve, M.; Verdaguer, M.; Gleizes, A.; Philoche-Levisalles, M.; Kahn, O. *Inorg Chem*. **1984**, *23*, 3808.

(13) (a) Julve, M.; Verdaguer, M.; Kahn, O.; Gleizes, A.; Philoche-Levisalles, M. *Inorg. Chem*. **1983**, *22*, 368. (b) Soto, L.; Garcia-Lozano, J.; Escriva, E.; Legros, J. P.; Tuchagues, J. P.; Dahan, F.; Fuertes, A. *Inorg. Chem*. **1989**, *28*, 3378. (c) Soto, L.; Garcia-Lozano, J.; Escriva, E.; Beneto, M.; Dahan, F.; Tuchagues, J. P.; Legros, J. P. *J. Chem. Soc., Dalton Trans.* **1991**, 2619.

(14) Charlot, M. F.; Verdaguer, M.; Journaux, Y.; de Loth, P.; Daudey, J. P. *Inorg. Chem.* **1984**, *23*, 3802.

(15) Alvarez, S.; Julve, M.; Verdaguer, M. *Inorg. Chem*. **1990**, *29*, 4500.

(16) Cano, J.; Alemany, P.; Alvarez, S.; Verdaguer, M.; Ruiz, E. *Chem. Eur. J*. **1998**, *4*, 476.

(17) (a) Anderson, P. W. *Phys. Rev*. **1959**, *2*, 115. (b) Anderson, P. W. *In Theory of the Magnetic Interaction: exchange in insulators and superconductors*; Seitz, F.; Turnbul, D., Eds.; Solid State Physics, Vol. 14; Academic Press: New York, 1963; pp 99−124.

(18) (a) Miralles, J.; Daudey, J. P.; Caballol, R. *Chem. Phys. Lett*. **1992**, *198*, 555. (b) Castell, O.; Miralles, J.; Caballol, R. *Chem. Phys.* **1994**, *179*, 377.

(19) Handrick, K.; Malrieu, J. P.; Castell, O. *J. Chem. Phys*. **1994**, *101*, 2205.

(20) Castell, O.; Caballol, R.; Subra, R.; Grand, A. *J. Phys. Chem*. **1995**, *99*, 154.

(21) Castell, O.; Caballol, R.; Garcia, V. M.; Handrick, K. *Inorg. Chem.* **1996**, *35*, 1609.

(22) Castell, O.; Caballol, R. *Inorg. Chem*. **1999**, *38*, 668.

(23) (a) Miralles, J.; Castell, O.; Caballol, R.; Malrieu, J. P. *Chem. Phys*. **1993**, *172*, 33. (b) Castell, O.; García, V. M.; Bo, C.; Caballol, R. *J. Comput. Chem*. **1996**, *17*, 42. (c) García, V. M.; Castell, O.; Caballol, R.; Malrieu, J. P. *Chem. Phys. Lett*. **1995**, *238*, 222. (d) García, V. M.; Castell, O.; Reguero, M.; Caballol, R. *Mol. Phys*. **1996**, *87*, 1395. (e) García, V. M.; Caballol, R.; Malrieu, J. P. *Chem. Phys. Lett*. **1996**, *261*, 98. (f) García, V. M.; Reguero, M.; Caballol, R. *Theor. Chem. Acc*. **1997**, *98*, 50. (g) García, V. M.; Caballol, R.; Malrieu, J. P. *J. Chem. Phys.* **1998**, *109*, 504−511.

(24) Cabrero, J.; Ben Amor, N.; Caballol, R. *J. Phys. Chem. A* **1999**, *103*, 6220.

(25) Illas, F.; Casanovas, J.; García-Bach, M. A.; Caballol, R.; Castell, O. *Phys. Rev. Lett*. **1993**, *71*, 3549.

(26) Casanovas, J.; Rubio, J.; Illas, F. *Phys. Rev. B* **1996**, *53*, 945.

(27) de Graaf, C.; Illas, F.; Broer, R.; Niewport, W. C. *J. Chem. Phys.* **1997**, *106*, 3287.

(28) Caballol, R.; Castell, O.; Illas, F.; Moreira, I.de P. R.; Malrieu, J. P. *J. Phys. Chem. A* **1997**, *101*, 7860.

(29) Illas, F.; Moreira, I. de P. R.; de Graaf, C.; Barone, V. *Theor. Chem. Acc.* **2000**, *104*, 265.

(30) (a) Martin, R. L.; Illas, F. *Phys. Rev. Lett*. **1997**, *79*, 1539. (b) Illas, F.; Martin, R. L. *J. Chem. Phys.* **1998**, *108*, 2519. (c) de Graaf, C.; Moreira, I. de P. R.; Illas, F.; Martin, R. L. *Phys. Rev. B* **1999**, *60*, 3457.

(31) (a) Calzado, C. J.; Sanz, J. F.; Malrieu, J. P. *J. Chem. Phys*. **2000**, *112*, 5158. (b) Calzado, C. J.; Sanz, J. F.; Malrieu, J.-P.; Illas, F. *Chem. Phys. Lett*. **1999**, *307*, 102. (c) Moreira, I. de P. R.; Illas, F.; Calzado, C. J.; Sanz, J. F.; Malrieu, J. P.; Ben Amor, N.; Maynau, D. *Phys. Rev. B* **1999**, *59*, R6593.

(32) Andersson, K.; Blomberg, M. R. A.; Fülscher, M. P.; Karlström, G.; Lindh, R.; Malmqvist, P. Å.; Neogrády, P.; Olsen, J.; Roos, B. O.; Sadlej, A. J.; Schütz, M.; Seijo, L.; Serrano-Andrés, L.; Siegbahn, P. E. M.; Widmark, P. O. MOLCAS, Version 4; Lund University: Lund, Sweden, 1997.

(33) Caballol, R.; Malrieu, J. P. *Chem. Phys. Lett.* **1992**, *188*, 543.

(34) DDCI program: Castell, O. (1995); CT version, Caballol, R. (1999); SCIEL program, Caballol, R.; Malrieu, J. P.; Daudey, J. P.; Castell, O. (1998).

(35) Román, P.; Guzmán-Miralles, C.; Luque, A.; Beitia, J. I.; Cano, J.; Lloret, F.; Julve, M.; Alvarez, S. *Inorg. Chem*. **1996**, *35*, 3741.

(36) Becke, A. D. *J. Chem. Phys.* **1993**, *98*, 5648.

(37) Frisch, M. J.; Trucks, G. W.; Schlegel, H. B.; Scuseria, G. E.; Robb, M. A.; Cheeseman, J. R.; Zakrzewski, V. G.; Montgomery, J. A.; Stratmann, R. E.; Buran, J. C.; Dapprich, S.; Millam, J. M.; Daniels, A. D.; Kudin, K. N.; Strain, M. C.; Farkas, O.; Tomasi, J.; Barone, V.; Cossi, M.; Cammi, R.; Mennucci, B.; Pomelli, C.; Adamo, C.; Clifford, S.; Ochterski, J.; Petersson, G. A.; Ayala, P. Y.; Cui, Q.; Morokuma, K.; Malick, D. K.; Rabuk, A. D.; Raghavachari, K.; Foresman, J. B.; Cioslowski, J.; Ortiz, J. V.; Stefanov, B. B.; Liu, G.; Liashenko, A.; Piskorz, P.; Komaromi, I.; Gomperts, R.; Martin, R. L.; Fox, D. J.; Keith, T.; Al-Laham, M. A.; Peng, C. Y.; Nanayakkara, A.; González, C.; Challacombe, M.; Gill, P. M. W.; Johnson, B. G.; Chen, W.; Wong, M. W.; Andrés, J. L.; Head-Gordon, M.; Replogle, E. S.; Pople, J. A. *Gaussian98*, Revision A.1; Gaussian, Inc.: Pittsburgh, PA, 1998.

(38) (a) Barone, V.; Gillon, B.; Plantevin, O.; Cousson, A.; Mathonière, C.; Kahn, O.; Grand, A.; Öhrström, L.; Delley, B. *J. Am. Chem. Soc.* **1996**, *118*, 11822. (b) Baron, V.; Gillon, B.; Cousson, A.; Mathonière, C.; Kahn, O.; Grand, A.; Öhrström, L.; Delley, B.; Bonnet, M.; Boucherle, J. X. *J. Am. Chem. Soc.* **1997**, *119*, 3500.

(39) The B3LYP *J* on this complex was reported by Cano et al. to be −41 cm^{-1}. Since the authors used the limit $S_{ab} = 1$ in eq 6, the present result is in agreement with it.

(40) Chevreau, H.; Moreira, I. de P. R.; Silvi, B.; Illas, F. Submitted for publication.